

Dependence on the Mobile-Phase pH of the Adsorption Behavior of Propranolol Enantiomers on a Cellulase Protein Used as the Chiral Selector

Torgny Fornstedt,[†] Gustaf Götmar,[†] Marie Andersson,[†] and Georges Guiochon^{**‡}

Contribution from the Department of Pharmacy, BMC, Box 580, S-751 23 Uppsala, Sweden, Department of Chemistry, University of Tennessee, Knoxville, Tennessee 37996-1600, and Division of Chemical and Analytical Sciences, Oak Ridge National Laboratory, Oak Ridge, Tennessee 37831

Received August 31, 1998

Abstract: We reported previously on the unusual thermodynamic characteristics of the enantioselective interactions between the enantiomers of the β -blocker propranolol and the protein cellobiohydrolase I immobilized on silica. The adsorption of the more retained enantiomer, (*S*)-propranolol, is endothermic while that of the (*R*)-propranolol is exothermic. This causes a rapid increase of the selectivity factor with increasing temperature. In this work, we study the complex dependence of the selectivity factor on the pH of the solvent. We determined the equilibrium isotherms of (*R*)- and (*S*)-propranolol in a wide concentration range (0.25 μ M to 1.1 mM) at six different mobile-phase pHs (4.7, 5.0, 5.2, 5.5, 5.7, and 6.0) and fitted the data obtained to the bi-Langmuir model. This gave the saturation capacity and the binding constant of the nonselective contribution for the two enantiomers. It also gave these parameters for the enantioselective contributions of each of them. The dependence of these parameters on the pH is discussed and interpreted in terms of the retention mechanism. Our conclusions are in excellent agreement with recent, independent results on the structure of the protein obtained by X-ray crystallography.

Introduction

Many pharmaceuticals are chiral. Although most of their physicochemical properties are identical (except for their interactions with polarized light and with other enantiomers), the two enantiomers of the same chiral drug may have different physiological effects and different metabolic and pharmacokinetic behaviors. As reported earlier by Howe and Shanks¹ and noted recently in an FDA policy statement,² the two enantiomers of several β -receptor antagonists, a group of amino alcohols with a chiral center, exhibit often different pharmacological and metabolic behaviors. For example, D-sotalol generates arrhythmic cardiac behavior, while L-sotalol is a β -blocker, and D-propranolol shows no β -blocking effects, while L-propranolol is an efficient β -blocker.² Therefore, it is important to be able to separate these enantiomers, whether for analytical or for production purposes.

HPLC is a most suitable separation method for this purpose, provided proper chiral stationary phases are available.^{3,4} The development of such phases has been rapid during the past decade. Much effort has been made to classify these new phases according to which groups or families of chiral drugs they can separate. Libraries or databases have been built up.⁵ Most investigations in this area originate, however, from experts in

chiral properties and their viewpoint is seldom that of the chromatographers. For example, although it has been abundantly validated,^{6–10} the concept that two retention mechanisms are mixed in chiral separations by chromatography has not yet been widely accepted.¹¹ Retention factors and even isotherms are still often treated as if only the selective retention mechanism was involved,^{11–16} although such an occurrence is highly improbable. More fundamental studies of the thermodynamics and mass transfer kinetics of the retention mechanisms of chiral phases are needed for a better understanding of the chiral recognition mechanisms.

One of the most important type of chiral stationary phases (CSPs) includes those obtained by chemically bonding a chiral ligand to the surface of a solid support, e.g., porous silica. Often, the ligand is a compound of natural origin and proteins are among the most popular.^{17,18} The interactions that take place

(6) Jacobson, S. C.; Golshan-Shirazi, S.; Guiochon, G. *J. Am. Chem. Soc.* **1990**, *112*, 6492.

(7) Jacobson, S. C.; Golshan-Shirazi, S.; Guiochon, G. *AIChE J.* **1992**, *37*, 836.

(8) Charton, F.; Guiochon, G. *J. Chromatogr.* **1993**, *630*, 21.

(9) Guiochon, G.; Golshan-Shirazi, S.; Katti, A. M. *Fundamentals of Preparative and Nonlinear Chromatography*; Academic Press: Boston, MA, 1994.

(10) Fornstedt, T.; Sajonz, P.; Guiochon, G. *J. Am. Chem. Soc.* **1997**, *119*, 1254.

(11) Ringo, M. C.; Evans, C. E. *Anal. Chem.* **1998**, *70*, 315A.

(12) Yang, J.; Hage, D. S. *J. Chromatogr., A* **1996**, *725*, 273.

(13) Loun, B.; Hage, D. S. *Anal. Chem.* **1994**, *66*, 3814.

(14) Wainer, I. W. *J. Chromatogr., A* **1994**, *666*, 221.

(15) Noctor, T. A. G.; Felix, G.; Wainer, I. W. *Chromatographia* **1991**, *31*, 55.

(16) Jönsson, S.; Schön, A.; Isaksson, R.; Pettersson, C.; Pettersson, G. *Chirality* **1992**, *4*, 505.

(17) Allenmark, S. *Chromatographic Enantioseparation*; Ellis Horwood, Chichester, U.K., 1991.

[†] BMC.

[‡] University of Tennessee and Oak Ridge National Laboratory.

(1) Howe, R.; Shanks, R. G. *Nature* **1966**, *210*, 1336.

(2) *Chirality* **1992**, *4*, 338.

(3) Pirkle, W. H.; Finn, J. Chiral High-Pressure Liquid Chromatographic Stationary Phases. *J. Org. Chem.* **1981**, *46*, 2935.

(4) Armstrong, D. W.; Han, S. M. Enantiomeric Separations in Chromatography. *CRC Crit. Rev. Anal. Chem.* **1988**, *19*, 175.

(5) CHIRBASE Project. ENSSPICAM, Université de Aix-Marseille III, Marseille, France.

between the bonded protein molecules and the analytes are similar to the drug-receptor interactions taking place in the body since receptors are proteins. As an example, one of the most successful proteins used as chiral selector is α_1 -acid glycoprotein, a human plasma protein.^{19,20} Commercialized under the name Chiral AGP, it is most likely the CSP with the broadest applicability.²⁰ However, cellobiohydrolase I (CBH I) immobilized on porous silica is preferred for the separation of basic chiral drugs containing one or more basic nitrogen atoms and one or more hydrogen-acceptor or hydrogen-donor groups.^{21,22} CBH I gives probably the best results and the largest separation factors for almost all the enantiomeric pairs of β -receptor antagonists (amino alcohols). For these separations, it gives larger separation factors than α_1 -acid glycoprotein.

CBH I is a cellulase enzyme, catalyzing the sequential removal of cellobiose units from the nonreducing end of the cellulose molecule.^{23,24} It exhibits product inhibition, its activity decreasing in the presence of increasing concentration of cellobiose.²³ When cellobiose was added to the mobile phase, the enantioselectivity was reduced, suggesting that the enzymatically active site and the chiral adsorption site overlap.^{25,26} The enzymatically active site contains several β -sheets and α -helical segments arranged to form an extended flat tunnel (ca. 40 Å long) into which the cellulose chain can be threaded and cleaved.^{23,24} Recent crystallographic studies suggest that the carboxylic groups from three amino acid residues, two from glutamic acid and one from aspartic acid, are important for the catalytic effect.²³ This was confirmed by kinetic studies made with the wild-type CBH I and with different mutant proteins in which these amino acids were replaced by glutamine.²⁷ Chromatographic experiments were made using immobilized mutant proteins and the immobilized wild-type CBH I as stationary phases. It was found that the loss of chiral recognition followed the same pattern as the loss of catalytic activity.^{28,29} The carboxylic groups of the two glutamic acids were found to be most important. It was suggested that they face each other, on both sides of the protonated nitrogen group of propranolol. There are two tryptophan residues, both at a suitable distance for interaction with the aromatic part of the β -blocker, which is also believed to play a role in the chiral recognition. At least one of them could interact with the naphthyl group of (*S*)-propranolol.

In recent publications we investigated the unusual temperature dependence of the retention time of (*S*)-propranolol (at pH = 5.5, it increases with increasing temperature, while that of (*R*)-propranolol decreases; at pH = 4.7, both retention times decrease with increasing temperature)¹⁰ and the unusually low efficiency and strong peak tailing observed for the more retained (*S*)-

propranolol and not for the less retained (*R*)-propranolol.³⁰ Satisfactory answers could be obtained by measuring the adsorption isotherms of the two enantiomers, separating the chiral and achiral mechanisms of retention, and using the rate theory of chromatography to model their band profiles.^{10,30} The theory of linear chromatography, conventionally used in such studies so far, does not allow such an intimate investigation of the chiral retention mechanism.^{16,22}

The most significant result of our earlier study was a demonstration of the strong pH dependence of the retention mechanisms (at pH = 4.7, the temperature effect indicated above was not observed).¹⁰ The goal of this study is to provide a better understanding of this behavior by discussing the results of an investigation of the dependence of the retention of the two propranolol enantiomers on CBH I on temperature and on the mobile-phase pH.

Theory

1. Adsorption Model. We have previously validated a simple adsorption model that accounts well for the interactions of enantiomers with immobilized proteins, such as BSA or CBH I, bonded to the surfaces of porous silica particles.⁶⁻¹⁰ The surfaces of these CSPs are heterogeneous, which affects both the thermodynamics and the kinetics of adsorption. Most of the adsorption sites found on these surfaces are nonselective. These sites, called here type-I sites, have identical behaviors toward the two enantiomers. They involve the exposed part of the silica surface, the residual Si-OH groups after bonding the enantiomeric selectors, and the achiral parts of these selectors. Although all the molecular interactions involving type-I sites have a low energy, their total contribution to the retention of the enantiomers is significant because of the large number of these sites. The low interaction energy of type-I sites explains their fast exchange kinetics. Thus, although type-I sites constitute a broad continuum, they can be characterized by an average adsorption energy and an average mass transfer coefficient and there is no practical way to determine the adsorption energy distribution.³¹

The enantioselective sites, called type-II sites, are specific regions of the bonded ligand (i.e., the protein) which are responsible for the chiral recognition. Their interactions with the two enantiomers require the strict fulfillment of some steric conditions. If these interactions are sufficiently enantioselective, they lead to the chiral separation. Type-II sites are few, much less numerous than type-I sites, but their energy of interaction with the enantiomeric analytes (or at least with one of them) is much stronger than that of type-I sites. Thus, in favorable cases, the contributions of type-I and type-II site interactions to the overall retention are comparable. Both types of site contribute to retention, but only type-II sites contribute to chiral resolution. In most cases, it seems that type-II sites adsorb both enantiomers, albeit one of them preferentially. In some cases,³² it has been demonstrated that they do not adsorb one of them. It is conceivable that two types of chiral type-II sites, one selective for the first enantiomer and the other for the second one, coexist on the surface. This situation has not yet been exemplified.

2. Retention Factors. The retention factor, derived from the elution peak of an infinitely small amount of the corresponding enantiomer (linear chromatography), is the sum of the contributions of the type-I and the type-II sites to the retention. Thus,

(18) Allenmark, S.; Andersson, S. *J. Chromatogr., A* **1994**, *666*, 167.

(19) Hermansson, J. *J. Chromatogr.* **1985**, *325*, 379.

(20) Hermansson, J. *TrAc* **1989**, *8*, 251.

(21) Marle, I.; Erlandsson, P.; Hansson, L.; Isaksson, R.; Pettersson, C.; Pettersson, G. *J. Chromatogr.* **1991**, *586*, 233.

(22) Isaksson, R.; Pettersson, C.; Pettersson, G.; Jönsson, S.; Ståhlberg, J.; Hermansson, J.; Marle, I. *TrAc* **1994**, *13*, 431.

(23) Divne, C.; Ståhlberg, J.; Reinikainen, T.; Ruohonen, L.; Pettersson, G.; Knowles, J. K. C.; Teeri, T. T.; Jones, T. A. *Science* **1994**, *265*, 524.

(24) Divne, C.; Ståhlberg, J.; Teeri, T. T.; Jones, T. A. *J. Mol. Biol.* **1998**, *275*, 309.

(25) Mohammad, J.; Li, Y.-M.; El-Ahmad, M.; Nakazato, K.; Pettersson, G.; Hjertén, S. *Chirality* **1993**, *5*, 464.

(26) Fornstedt, T.; Hesselgren, A.-M.; Johansson, M. *Chirality* **1997**, *9*, 329.

(27) Ståhlberg, J.; Divne, C.; Koivula, A.; Piens, K.; Claeysens, M.; Teeri, T. T.; Jones, T. A. *J. Mol. Biol.* **1996**, *264*, 337.

(28) Henriksson, H.; Ståhlberg, J.; Isaksson, R.; Pettersson, G. *FEBS Lett.* **1996**, *390*, 339.

(29) Henriksson, H.; Ståhlberg, J.; Koivula, A.; Pettersson, G.; Divne, C.; Valtcheva, L.; Isaksson, R. *J. Biotechnol.* **1997**, *57*, 115.

(30) Fornstedt, T.; Zhong, G.; Benseititi, Z.; Guiochon, G. *Anal. Chem.* **1996**, *68*, 2370.

(31) Rudzinski, W.; Everett, D. H. *Adsorption of Gases on Heterogeneous Surfaces*; Academic Press: New York, 1992.

(32) Chen, Y.; Kele, M.; Sajonz, P.; Sellergren, B.; Guiochon, G. *Anal. Chem.* In press.

the overall retention factors for enantiomers 1 and 2, are respectively

$$k'_1 = k'_{1,I} + k'_{1,II} \quad (1a)$$

$$k'_2 = k'_{2,I} + k'_{2,II} \quad (1b)$$

The Roman figures stand for the types of sites and the Arabic ones for the enantiomers. Since type-I sites are achiral, $k'_{1,I} = k'_{2,I}$ and the number of unknown parameters in the two equations can be reduced to 3. Still, it is impossible to identify these three contributions from the only parameters that can be measured in linear chromatography, the two retention factors in eqs 1a,b, k'_1 and k'_2 . The only correct method to determine these three contributions is the acquisition of the nonlinear adsorption isotherms.^{9,10}

3. Adsorption Isotherms. An adsorption isotherm relates the concentrations of a compound in the two phases in equilibrium (here, the stationary and the mobile phase), at constant temperature. The Langmuir equation is the simplest model of a nonlinear isotherm. It accounts well for the adsorption of single components on homogeneous surfaces, at low and moderate concentrations, or for the isolated adsorption of a solute on either type-I or type-II sites, respectively. This model is expressed by the classical equation

$$\theta = \frac{q}{q_s} = \frac{bC}{1 + bC} = \frac{\Gamma}{1 + \Gamma} \quad (2)$$

where θ is the fraction of a monolayer covering the surface when it is in equilibrium with a concentration C in the mobile phase, q the corresponding stationary phase concentration, and q_s the concentration corresponding to a monolayer. The coefficient b (dimension of the reverse of a concentration) depends on the adsorption energy and the temperature. The product $\Gamma = bC$ characterizes the deviation of the isotherm from linear behavior. If Γ is negligible compared to unity, the isotherm behaves as if it were linear. If Γ is large, the isotherm deviates markedly from linear behavior. The accurate determination of the isotherm parameters requires that measurements of θ be performed in a broad range of concentration values, from very small values of Γ (i.e., infinite dilution) to values of Γ large or at least significant compared to unity. The classical retention factor at infinite dilution is related to the numerical coefficients of the Langmuir isotherm by

$$k' = F \frac{\partial q}{\partial C} = Fq_s b = Fa \quad (3)$$

where $a = bq_s$ is the equilibrium or Henry constant, i.e., the initial slope of the adsorption isotherm, and F the phase ratio (with $F = (1 - \epsilon)/\epsilon$, where ϵ is the total porosity of the column).

The contributions of type-I and type-II sites to the adsorption isotherm are independent and additive. Thus, the adsorption isotherms of both enantiomers are the sum of two terms, accounting for the contributions of the two types of sites, type-I and type-II sites, respectively. These isotherms are accounted for by the bi-Langmuir model

$$q_1 = q_{1,I} + q_{1,II} = \frac{q_{1,I,s} b_{1,I} C_1}{1 + b_{1,I} C_1} + \frac{q_{1,II,s} b_{1,II} C_1}{1 + b_{1,II} C_1} \quad (4a)$$

$$q_2 = q_{2,I} + q_{2,II} = \frac{q_{2,I,s} b_{2,I} C_2}{1 + b_{2,I} C_2} + \frac{q_{2,II,s} b_{2,II} C_2}{1 + b_{2,II} C_2} \quad (4b)$$

This model is the simplest one available to describe adsorption

on a heterogeneous surface of the type encountered in chiral separations. Because of Pasteur principle, the contributions of the achiral type-I sites to the isotherms of the two enantiomers are the same; hence, $b_{1,I} = b_{2,I}$ and $q_{1,I,s} = q_{2,I,s}$. Hence, the set of eqs 4a,b contains usually six parameters only, instead of eight. This model has been used successfully to describe the adsorption behavior of many pairs of enantiomers on different CSPs.⁶⁻¹⁰

From eqs 3 and 4, the retention factors at infinite dilution of the two enantiomers are

$$k'_1 = k'_{1,I} + k'_{1,II} = F(q_{1,I,s} b_{1,I} + q_{1,II,s} b_{1,II}) = F(a_{1,I} + a_{1,II}) \quad (5a)$$

$$k'_2 = k'_{2,I} + k'_{2,II} = F(q_{2,I,s} b_{2,I} + q_{2,II,s} b_{2,II}) = F(a_{2,I} + a_{2,II}) \quad (5b)$$

with $k'_{1,I} = k'_{2,I}$ (Pasteur principle). Since type-II sites are much fewer than type-I sites, $q_{i,I,s} \gg q_{i,II,s}$. Because the adsorption energy is much larger on type-II sites than on type-I sites, $b_{i,II} \gg b_{i,I}$. This explains why $a_{1,I}$ and $a_{1,II}$ turn out to be of comparable magnitude in many cases. When the former is much larger than the latter, there is retention but little or no enantioselectivity and no enantiomeric separation.

The three contributions, $k'_{1,I} = k'_{2,I}$, $k'_{1,II}$, and $k'_{2,II}$, can be derived from the isotherm data of the two enantiomers. Thus, it is possible to characterize a CSP by two separation factors. The first such factor is the apparent separation factor, $\alpha_{app} = k'_2/k'_1$, which measures the actual difficulty of the chromatographic separation. The second factor is the true enantiomeric separation factor, $\alpha_{true} = k'_{2,II}/k'_{1,II}$. Only the latter value is meaningful for a discussion of the mechanism of enantioselectivity.

Finally, the relative density of the sites of either type on the surface can be derived from the best parameters of the isotherms. We have $q_j = q_{j,s}/(q_{j,I,s} + q_{j,II,s})$, with q_j being the relative abundance of type- j sites on the surface. Note that the results for the two compounds may be slightly different as $q_{1,II,s}$ and $q_{2,II,s}$ are slightly different.

Experimental Section

1. Apparatus. The data were obtained with a Shimadzu LC-10 system (Shimadzu, Kyoto, Japan) equipped with two pumps, an autoinjector, a UV detector, and a data station controlling the equipment and acquiring the data. The outlets of the two pumps were connected directly, with a low-dead-volume PEEK tee. All connections among the tee, the column, and the flow cell were made with 0.17 mm PEEK capillaries. The column was placed in a laboratory-assembled column jacket and temperature controlled using an MN6 Lauda circulating water bath (Lauda, Königshofen, Germany).

2. Chemicals. (*R*)-(+)-Propranolol and (*S*)-(-)-propranolol (the active β -blocking enantiomer) were 99% pure chemicals from Sigma Chemicals (St. Louis, MO). The buffer salts were acetic acid (>99.8%) and anhydrous sodium acetate (>99%) from Riedel-de Haën (Seelze, Germany). The water used was from Millipore, MilliQ grade. After dissolution of the buffer salts, the stock solutions were filtered on 0.45 μ m filters (Kebo, Spånga, Sweden).

3. Column and Immobilization of the Stationary Phase. The protein cellobiohydrolase I, CBH I, was immobilized on silica particles, as described previously.¹⁰ The material obtained was packed in a 100 \times 4.6 mm stainless steel column. The concentration of the CBH I immobilized on the silica support was determined by measuring the UV absorbance at 280 nm of the solution used, before and after its reaction with aldehyde silica. The amount of protein bonded to the diol silica was found to be 50.7 mg/g of packing. The amount of protein in the column, 45.6 mg, was derived from the bonded protein/diol silica concentration and from the dry weight of packing material in the column.

Table 1. Analytical Retention and Separation Factors of (*R*)- and (*S*)-Propranolol at Different Mobile-Phase pHs and Temperatures (Ionic Strength $I = 0.02$ M)

pH	T (°C)	k'_R	k'_S	α
4.73	10	3.57	4.14	1.16
	20	2.85	3.67	1.29
	30	2.27	3.25	1.43
	40	1.84	2.90	1.58
4.98	10	4.63	5.60	1.21
	20	3.62	4.97	1.37
	30	2.94	4.60	1.56
	40	2.41	4.25	1.76
5.21	10	5.90	7.51	1.27
	20	4.63	6.85	1.47
	30	3.78	6.56	1.73
	40	3.10	6.22	2.01
5.56	10	7.94	11.09	1.40
	20	6.41	11.01	1.72
	30	5.31	11.06	2.08
	40	4.47	10.99	2.46
5.74	10	8.98	13.09	1.46
	20	7.31	13.21	1.81
	30	6.21	13.61	2.19
	40	5.22	13.82	2.65
6.00	10	11.00	17.22	1.57
	20	9.13	18.37	2.01
	30	7.83	19.77	2.52
	40	6.81	20.76	3.05

4. Mobile Phase. Solutions of an acetic buffer at six different pH values between 4.7 and 6.0 were used as the mobile phase. All these solutions contained 20.0 mM sodium acetate, and the ionic strength of the mobile phase was kept constant at $I = 0.02$. The concentration of acetic acid was calculated to achieve the desired pH value, using the Henderson–Hasselbalch equation. The exact pH was measured with a calibrated Metrohm 632 pH meter (Metrohm, Herisau, Switzerland). The mobile-phase flow rate was 1.00 mL/min. The exact pH values of the solutions used are reported in Tables 1 and 2.

5. Procedures. Frontal analysis in the staircase mode was used to determine the adsorption isotherms of the two propranolol enantiomers.^{9,10} Pure mobile phase was used as the solvent in pump A and a solution of suitable concentration of one of the two enantiomers as the solvent in pump B. The solute concentration in the eluent was increased stepwise, by programming the system controller in the high-pressure gradient mode to execute step gradients at the appropriate time. Data points are required in a broad concentration range in order to obtain sufficient accuracy in the estimates of the contributions of the low-capacity enantioselective sites and the high-capacity nonselective sites, respectively. Three solutions of each enantiomer were used successively as solvent B, allowing the determination of the isotherm data in the concentration range between 0.25 μ M and 1.1 mM, an approximately 4400-fold dynamic range. An isotherm was acquired for each enantiomer, R and S propranolol at each of six different pH values. Each isotherm contained 26 data points with concentrations between 0.25 μ M and 1.1 mM.

Two wavelengths were used for the UV detection, 230 and 254 nm, depending on the actual concentration. The column hold-up volume, V_0 , was determined to be 1.26 mL, derived from the elution time of the first buffer/water disturbance peak. The hold-up volume did not change with the pH values used in this study. All the frontal analysis data were corrected for the dead-volume contribution of the instrument and for the column hold-up volume. The total correction volume, V_c , was determined to be 1.58 mL (V_0 is included in V_c).

The best values of the parameters of the bi-Langmuir isotherm (eqs 4a,b) were calculated using a nonlinear regression method, the Gauss–Newton algorithm with the Levenberg modification as implemented in the software PCNONLIN 4.2 from Scientific Consulting (Apex, NC). In the regression, the experimental data were given a weight equal to $1/q_{\text{pred}}$, where q_{pred} is the stationary-phase concentration predicted by the model. This forces the program to tolerate the same relative error

Table 2. Bi-Langmuir Isotherm Parameters for (*R*)- and (*S*)-Propranolol at Different Mobile-Phase pHs (Ionic Strength $I = 0.02$)

type of site	pH	a	rsd ^a (%)	b (mM ⁻¹)	rsd ^a (%)	q_s (mM)
R,I	4.72	5.00	1.9	0.328	6.0	15.2
	4.98	6.10	1.8	0.364	5.2	16.8
	5.21	7.09	1.9	0.378	5.4	18.8
	5.49	7.76	2.8	0.354	7.6	21.9
	5.70	9.02	2.3	0.364	6.4	24.8
S,I	5.93	9.64	2.5	0.334	7.8	28.9
	4.72	4.65	2.9	0.297	8.3	15.7
	4.98	5.68	2.0	0.335	5.8	17.0
	5.21	6.97	1.4	0.393	4.2	17.7
	5.49	7.76	1.4	0.354	4.7	21.9
R,II	5.70	9.16	1.5	0.379	4.9	24.2
	5.93	10.33	1.5	0.392	4.9	26.4
	4.72	3.54	2.9	14.508	10.0	0.24
	4.98	4.85	2.6	16.287	8.9	0.30
	5.21	6.13	2.5	16.142	8.7	0.38
S,II	5.49	8.90	2.3	13.080	8.7	0.68
	5.70	11.20	2.0	15.131	7.2	0.74
	5.93	14.72	2.0	16.190	7.0	0.91
	4.72	6.65	1.6	9.834	6.4	0.68
	4.98	10.16	1.2	14.196	4.4	0.72
S,II	5.21	14.28	1.1	21.368	3.5	0.67
	5.49	22.41	1.2	28.788	3.1	0.78
	5.70	32.42	1.4	41.766	3.2	0.78
	5.93	44.58	1.5	57.773	3.3	0.77

^a rsd = relative standard deviation.

on each data point and avoids sacrificing the precision on the low-concentration data, which are important for linear chromatography.

Results and Discussion

1. Known Chromatographic Properties of Immobilized CBH I. Immobilized CBH I protein is a somewhat unusual CSP, with a narrow scope of application. It seems mostly able to separate the enantiomers of amino alcohols, such as β -receptor antagonists, but it can separate almost all of them with high selectivity factors. The best mobile phase is an aqueous buffer to which small amounts of an organic solvent such as 2-propanol or acetonitrile are added. The retention times of both β -blocker enantiomers increase with decreasing concentration of the organic modifier and with decreasing concentration of the buffer. The selectivity factor is strongly dependent on the mobile-phase pH and on the column temperature. The *S* enantiomer is always the more retained one. Its retention time increases more rapidly with increasing mobile-phase pH than that of the *R* enantiomer.

An unusual temperature effect was previously reported. It was found to be strongly dependent on the mobile-phase pH. When the column temperature increases at a mobile-phase pH of 5.5, the retention time of (*S*)-propranolol increases, which is most unusual. By contrast, at a mobile-phase pH of 4.7, the retention time of (*S*)-propranolol decreases, a conventional behavior, similar to that of the *R* enantiomer at both pH values. The selectivity factor increases with increasing temperature at both pH values, however, but less rapidly at pH = 4.7 than at pH = 5.5.

Finally, note that the amine group of propranolol ($pK_a = 9.5$) is protonated at all the pH values where measurements have been done. Thus the analyte (Figure 1) is always a cation under the experimental conditions of interest. It can give strong electrostatic interactions with the exposed ionized groups of the protein.

2. Properties of CBH I and Retention Mechanism. The pI of CBH I is close to 3.9. In the pH range of this study (4.7–

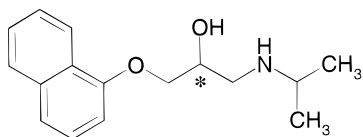


Figure 1. Structure of the chiral solute propranolol. The chiral center is marked with an asterisk.

6.0), its net charge is negative. It contains 43 amino acid residues with a carboxylic group, 24 being aspartic acid and 19 glutamic acid residues. The three-dimensional structure of CBH I was determined using X-ray protein crystallography. This showed an ~ 45 Å long tunnel within which the cellulose chain threads and is cleaved into cellobiose units. It is assumed that propranolol binds inside this tunnel, at the same site (the molecule loses most of its selectivity in the presence of cellobiose^{25,26}). Sixteen of the 43 amino acid residues with a carboxylic group are located inside the tunnel, 11 being aspartic acid and 5 glutamic acid residues. Two of these glutamic acid residues are borderline cases. In this tunnel, the acid groups of three amino acid residues (two from glutamic acid and one from aspartic acid) are critical for the enantioselective bonding of the enantiomers of propranolol. This was shown by the comparison of chromatograms obtained on silica bonded to either wild-type CBH I or different mutant proteins in the chain of which these amino acids are replaced by glutamine.²⁹ The carboxylic groups of the two glutamic acids were most important. It was suggested that they face each other and come on the two sides of the protonated nitrogen group of propranolol (see the structure of propranolol in Figure 1). There are also two tryptophan residues at a suitable distance for interaction with the aromatic part of propranolol to form a strong hydrophobic interaction. At least one of the tryptophan residues would stack to the naphthyl group of *S* propranolol (cf. Figure 1). The pK_a values of the carboxyl groups are usually between 3.5 and 4.5 in free amino acids. In acids incorporated in a protein molecule, this pK_a can be strongly perturbed, due to the microenvironment. It is usually quite larger, so all the carboxylic groups may not be dissociated in the low pH range of our study.

The pH dependence of retention, previously reported by Fornstedt et al.^{10,30} and confirmed by Henriksson et al.,²⁹ suggests that electrostatic interactions, most likely between the positively charged nitrogen of propranolol and one or more negatively charged carboxylic groups on the active site in the protein tunnel, are responsible for chiral recognition. This set of groups would constitute the type-II sites of this CSP. When the pH of the mobile phase is increased, from 4 to 6 or 7, the solute remains positively charged but more and more carboxylic acid residues at and around the type-II site become negatively charged. This causes the formation of a high negative charge in the protein tunnel. Although most of these interactions belong to the type-I sites, they also contribute to an increase in the energy of interaction with the type-II sites.

To elucidate further the enantioselective retention mechanism, it is necessary to acquire adsorption data for the propranolol enantiomers in the important pH range 4.7–6.0. This study has been conducted in two successive steps. First, a semiquantitative investigation of the influence of the column temperature and the mobile-phase pH on retention in linear elution chromatography was undertaken. Its purpose was to determine the extent of the transition range within which the selective adsorption of the *S* enantiomer changes from the exothermic, normal behavior to the unusual endothermic behavior previously reported at pH = 5.5. Second, a quantitative study was carried out, involving the determination of the adsorption isotherms by frontal analysis

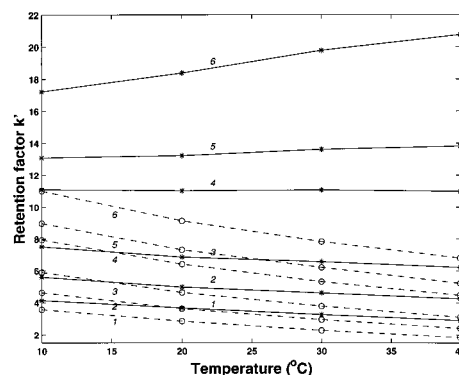


Figure 2. Retention factors of (*R*)- (circles, dashed lines) and (*S*)-propranolol (asterisks, solid lines) versus the column temperature at different pHs of the mobile phase. Conditions: column, 100×4.6 mm; stationary phase, immobilized CBH I on silica; eluent, acetic buffer at $I = 0.02$; mobile phase flow rate, 1.0 mL/min; sample, 20 μ L of 0.1 mM *rac*-propranolol. Mobile-phase pH: (1) 4.73; (2) 4.98; (3) 5.21; (4) 5.56; (5) 5.74; (6) 6.00.

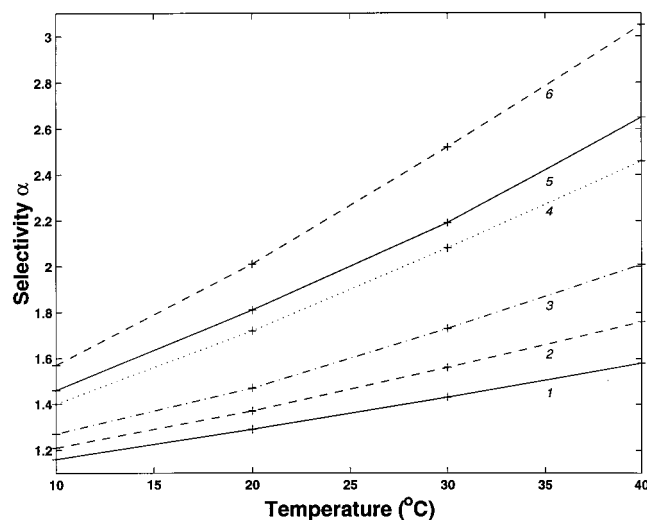


Figure 3. Selectivity factor, α , for *rac*-propranolol as a function of the temperature at different pHs of the mobile phase. The pH values are the same as those as in Figure 2. Data were taken from Table 1.

and the modeling of the experimental data using eqs 4a,b, to separate the contributions of the type-I and type-II sites at the different pH values. In the latter study, the temperature was kept constant at 25.0 °C.

3. Retention Factors in Linear Chromatography. The retention factors of the two enantiomers were measured systematically at six different mobile-phase pHs, between 4.7 and 6.0, and at four temperatures, between 10 and 40 °C. The results are reported in Figure 2 (symbols) and Table 1. At all values of the pH, the retention factor of (*R*)-propranolol (circles, dashed lines) decreases with increasing temperature. At each temperature, the retention factor of either enantiomer increases with increasing value of the pH. However, the retention factor of (*S*)-propranolol (asterisks, solid lines) decreases with increasing temperature only at pH ≤ 5.2 (lines 1–3 in Figure 2). At higher pH values, the retention factor increases with increasing temperature. The change in behavior is progressive; the average slope of plots of k' versus T in Figure 2 increases with increasing pH and goes through 0 around pH = 5.4. This behavior is also illustrated in Figure 3, which shows a plot of the separation factor versus the temperature at different mobile-phase pHs. The separation factor increases with both increasing pH and increasing temperature.

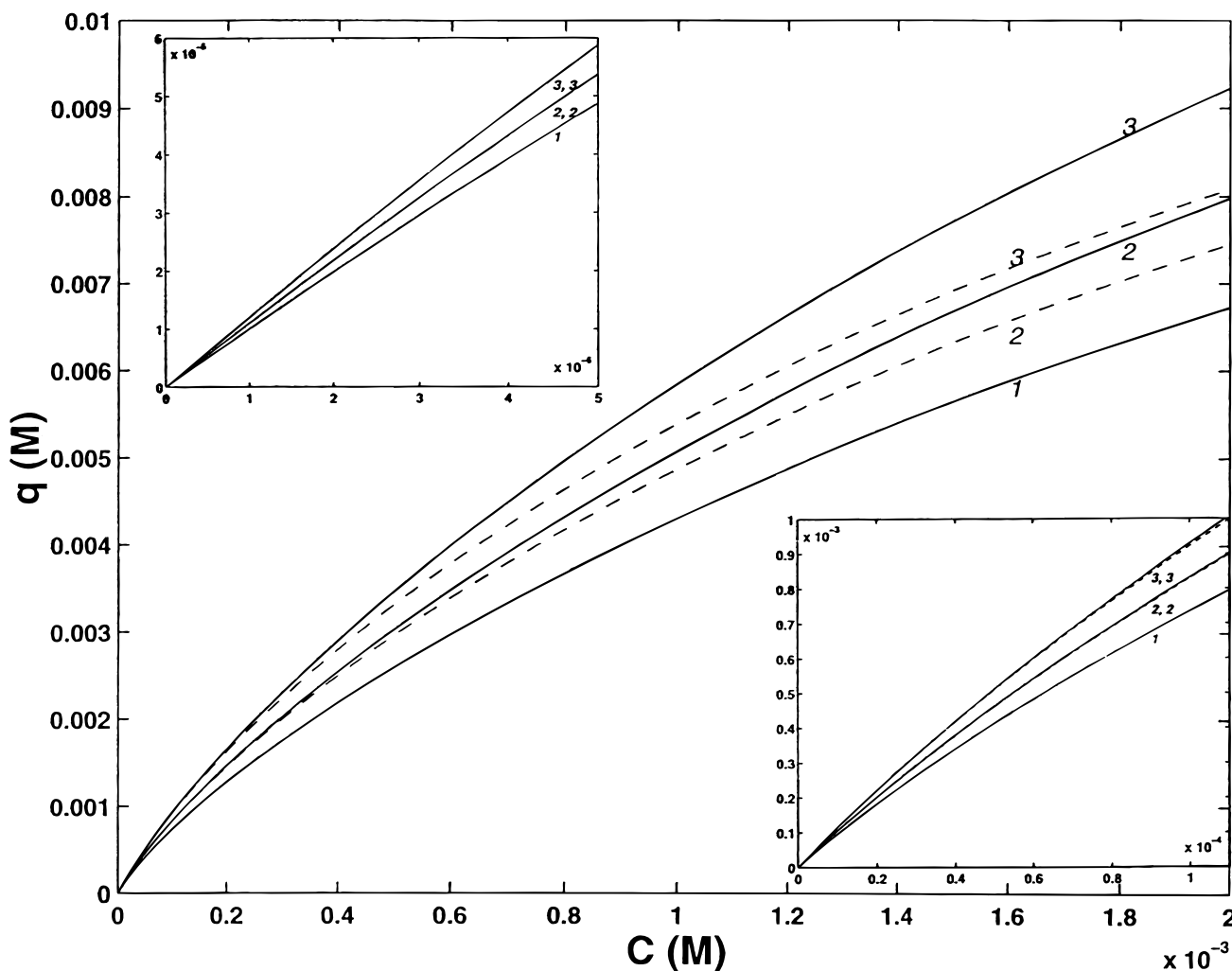


Figure 4. Comparison of bi-Langmuir isotherms calculated for different values of the type-I site parameters. The solid lines illustrate the case of increasing values of $q_{I,s}$ at a constant value of b_I (0.30 mM^{-1}): $q_{I,s}$ is (1) 16.7 mM, (2) 20.0 mM, (3) 23.3 mM. The dotted lines illustrate the case of increasing values of b_I at a constant value of $q_{I,s}$ (16.7 mM): b_I is (1) 0.30 mM^{-1} , (2) 0.36 mM^{-1} , (3) 0.42 mM^{-1} . The type-II parameters are both constant: $q_{II,s} = 0.5 \text{ mM}$ and $b_{II} = 10.0 \text{ mM}^{-1}$. The main figure shows the highest concentration range (mobile-phase concentrations between 0 and 2.0 mM). The top left inset shows the lowest concentration range (concentrations between 0 and 5 μM); in this figure the solid and dotted lines coincide. The bottom right inset shows the medium concentration range (concentrations between 0 and 0.1 mM).

Actually, however, as shown under Theory (see discussions of eqs 1 and 5), the retention factors measured in linear chromatography are the sums of two contributions. We know that, for both propranolol enantiomers, the nonselective contribution is exothermic. We know also that, at $\text{pH} = 5.5$, the enantioselective contribution for (*S*)-propranolol is endothermic.¹⁰ The combination of both contributions does not give much information. The apparent athermal behavior at pH around 5.5 (Figure 2) results from the balance between two opposite behaviors that cancel each other. The determination of the isotherm data is necessary to understand the chiral retention mechanism.

4. Adsorption Isotherms. For this section, each of two figures (Figures 4 and 5) contains a main figure corresponding to the large concentration range, 0–2 mM, and two insets, one in the top left corner corresponding to the low concentration range, 0–5 μM , and the other in the bottom right corner, corresponding to the medium concentration range, 0–0.1 mM. In the first subsection, we discuss the influence of the data in the different concentration ranges on the accuracy of the six different parameters to be determined. In later sections, we discuss the experimental results and their modeling.

a. Range of Concentration and Accuracy of the Param-

eters. The investigation of the influence of the pH on the isotherms of the two enantiomers is complex because the bi-Langmuir model contains the contributions of both type-I and type-II sites and, in principle at least, all the parameters a , b , and q_s of both contributions could be functions of the pH . In this study, it is of special interest to evaluate whether the saturation capacity, i.e., the number of the adsorption sites of each type (the q_s terms), varies with the pH and how their interaction energies (i.e., the b terms) change with the pH . A simulation of the fitting procedure allows a better understanding of the need to carry out experimental measurements in an unusually broad concentration range.

In Figure 4, we study on a theoretical basis the dependence of the isotherms on the contribution of type-I sites. In Figure 5, we do the same for the contribution of type-II sites. There are five isotherms in each figure. The solid lines in Figure 4 were calculated for slightly different values of the parameter $q_{I,s}$ (at constant b_I), while the dashed lines correspond to slightly different values of b_I (at constant $q_{I,s}$). The changes in these curves illustrate the sensitivity of the isotherms to changes in the values of the parameters. The effect of a parameter depends strongly on the concentration range investigated. The usefulness

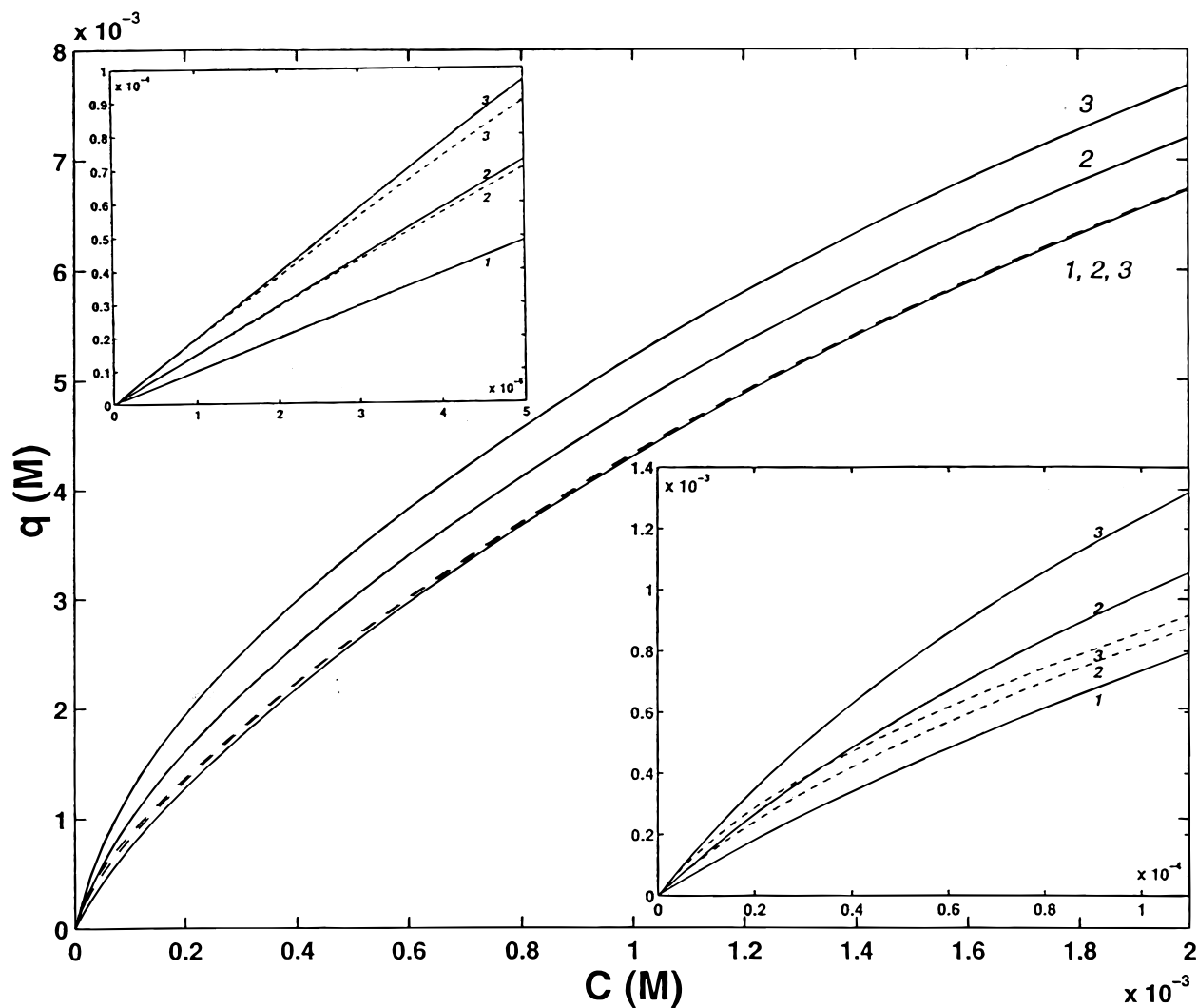


Figure 5. Comparison of bi-Langmuir isotherms calculated for different values of the type-II site parameters. The solid lines illustrate the case of increasing values of $q_{II,s}$ at a constant value of b_{II} (10.0 mM^{-1}): $q_{II,s}$ is (1) 0.5 mM , (2) 1.0 mM , (3) 1.5 mM . The dotted lines illustrate the case of increasing values of b_{II} at a constant value of $q_{II,s}$ (0.5 mM): b_{II} is (1) 10.0 mM^{-1} , (2) 20.0 mM^{-1} , (3) 30.0 mM^{-1} . The type-I parameters are both constant: $q_I = 16.7 \text{ mM}$ and $b_I = 0.30 \text{ mM}^{-1}$. The main figure shows the highest concentration range (mobile-phase concentrations between 0 and 2.0 mM). The top left inset shows the lowest concentration range (concentrations between 0 and $5 \mu\text{M}$). The bottom right inset shows the medium concentration range (concentrations between 0 and 0.1 mM).

of this study is that it will allow the determination of the concentration range within which data must be measured.

The initial type-I isotherm parameters were $b_I = 0.30 \text{ mM}^{-1}$ and $q_{I,s} = 16.7 \text{ mM}$ (i.e., $a_I = 5$), and those for type II were $b_{II} = 10.0 \text{ mM}^{-1}$ and $q_{II,s} = 0.5 \text{ mM}$ (i.e., $a_{II} = 5$; Figure 4, line 1). These values of the saturation capacity correspond to densities of 97.1% and 2.9% for type-I and type-II sites, respectively, well within the range previously reported for CBH I immobilized on a silica surface.¹⁰ Because $b_I C$ becomes larger than 0.10 for $C > 0.33 \text{ mM}$, the contribution of type-I sites to the isotherm has a nonlinear behavior only in the high concentration range (main figure). At the highest mobile phase concentration shown ($C_m = 2.0 \text{ mM}$), the surface coverage, θ_I , is approximately 40% and the type-I isotherm contribution is strongly nonlinear. By contrast, the contribution of type-II sites to the isotherm is linear only in the lowest concentration range (Figure 4, top left inset). It is already strongly nonlinear in the medium concentration range. The surface coverage of type-II sites becomes $\theta_{II} \sim 10\%$ for $C_m \sim 0.01 \text{ mM}$. It reaches 50% for the highest concentration in the bottom right inset of Figure 4. The curvature of the contribution of type-II sites is strong in the range covered by this inset. In the main figure, this

contribution is practically flat, the surface coverage at $C_m = 2.0 \text{ mM}$ being $\theta_{II} = 95\%$.

The other isotherms in Figure 4 were calculated with slightly different values of the parameters. The solid lines illustrate the effect of an increase of $q_{I,s}$, from 16.7 mM (line 1) to 20.0 mM (line 2) and to 23.3 mM (line 3), at a constant value of b_I (0.30 mM^{-1}). The dotted lines illustrate the effect of an increase of b_I , from 0.30 mM^{-1} (line 1) to 0.36 mM^{-1} (line 2) and to 0.42 mM^{-1} (line 3), at constant $q_{I,s}$ (16.7 mM). These values give 5.0, 6.0, and 7.0, respectively, for the product $a_I = b_I q_{I,s}$, i.e., for the Henry constant. In all cases, the parameters of the type-II isotherm contribution were kept constant.

Obviously, all isotherms being linear in the low concentration range, a variation of the saturation capacity, $q_{I,s}$, at constant b_I gives the same results as the same variation of b_I at constant $q_{I,s}$, i.e., the same isotherm. In both cases, the initial slope of the isotherm (eq 3) increases, as illustrated in the top inset of the figure. The corresponding solid and dotted lines coincide, and it is impossible to distinguish between the two contributions. In the medium concentration range (Figure 4, bottom inset), the type-II sites become strongly overloaded ($\theta_{II} = 52.4\%$ at $C_m = 0.11 \text{ mM}$). Nevertheless, the curvature of the isotherms

remains moderate because the proportion of the surface area occupied by these overloaded type-II sites is only 2.9%. The contribution of the type-I sites which represent 97.1% of the surface area is still nearly linear in this range, as explained above ($\theta_I \sim 3.3\%$ at $C_m = 0.11$ mM). Yet, this small contribution explains the slight tendency for a separation between the solid and dotted lines. In practice, however, it is not possible to use the isotherm data acquired in this range to distinguish between the effects of an increase of q_I and an increase in b_I . For data acquired in this range, the numerical problem of fitting the data to the eqs 4a,b would be ill-posed.

The precise determination of b_I and q_I becomes possible only when data are obtained in the highest concentration range, shown in the main Figure 4. In this last range, the isotherms are strongly nonlinear and there is a significant difference among the five calculated isotherms. It is only from the isotherm data acquired in this range that it is possible to determine a good estimate of the ordinate, $q_{I,s}$, of the asymptote. The main Figure 4 shows that, for a given value of the initial slope of the isotherm, increasing b_I increases the average curvature. This is because the saturation capacity ($q_{I,s} = a_I/b_I$) decreases and, since the product $b_I C$ increases, the curve gets closer to its horizontal asymptote. The converse is true for $q_{I,s}$, and all the dotted lines have the same asymptote. Finally, although the data acquired in the high concentration range allow the necessary distinction between the effects of $q_{I,s}$ and b_I (and, hence, permit their determination by parameter identification; see later), a degree of uncertainty remains on the estimate of $q_{I,s}$ since the corresponding type-I sites cannot be fully saturated.

A similar analysis can be made for the contribution of the type-II sites. The solid lines in Figure 5 illustrate the influence of an increase of $q_{II,s}$ (0.5 mM for line 1, 1.0 mM for line 2, and 1.5 mM for line 3), at constant b_{II} (10.0 mM⁻¹). The dotted lines illustrate that of an increase of b_{II} (10.0 mM⁻¹ for line 1, 20.0 mM⁻¹ for line 2, and 30.0 mM⁻¹ for line 3), at constant $q_{II,s}$ (0.5 mM). In all cases, the parameters of the contribution of type-I sites were kept constant ($q_{I,s} = 16.7$ mM and $b_I = 0.30$ mM⁻¹). In the lowest concentration range (Figure 5, top left inset), the solid lines coincide with the dotted lines in their initial parts since the isotherm contribution of type-II sites is practically linear at concentrations below 1 μ M ($b_{II} C = 1 \times 10^{-2}$, 2×10^{-2} , 3×10^{-2} , respectively; $\theta_{II} = 1\%$, 2% , 3%). At higher concentrations, a slight deviation can be seen, similar to the one observed in the bottom right inset of Figure 4, for type-I sites and for the same reason, the onset of nonlinear behavior. In this low concentration range, it is impossible to identify any of the parameters of the two isotherm contributions, not even the saturation capacity of type-II sites.

In the medium range of concentrations (Figure 5, bottom right inset), the isotherm contribution of the type-II sites is strongly nonlinear (surface coverage of type-II sites at $C_m = 0.11$ mM: $\theta_{II} = 52.4\%$ for $b_{II} = 10.0$ mM, 68.7% for $b_{II} = 20.0$ mM, and 76.7% for $b_{II} = 30.0$ mM). Under these conditions, an increase of $q_{II,s}$ at constant b_{II} is easily distinguished from an increase of b_{II} at constant $q_{II,s}$. The former (cf. solid lines) results in steeper isotherms, while the latter results in isotherms more strongly curved (cf. dotted lines). In the high concentration range (main Figure 5), the surface coverage of the type-II sites is very high ($\theta_{II} \sim 95\%$ – 98% , depending on the value of b_{II}) and the contribution of type-II sites is limited to a shift of the horizontal asymptote of the global isotherm.

In summary, the accurate determination of the parameters of a bi-Langmuir adsorption isotherm requires the acquisition of the experimental isotherm data in a dynamic concentration range

of at least 4000. The data in the low part of this concentration range provide the sum of the two a parameters (i.e., $a_I + a_{II}$; see eqs 5a,b) and a check on the linearity of the isotherm (i.e., it shows that the lowest concentrations studied were low enough). The data in the medium concentration range provide the strength of the adsorption energy on the type-II sites (i.e., the value of b_{II}) and an estimate of the saturation capacity, $q_{II,s}$. Finally, the data in the high concentration range give a confirmation of the estimate of $q_{II,s}$ and the parameters b_I and $q_{I,s}$.

b. Measurement of Adsorption Isotherm Data. In previous publications it was shown that the adsorption isotherm of propranolol was consistent with the bi-Langmuir adsorption model.^{10,30} This result agrees with the conclusions of our previous studies on another chiral selector, bovine serum albumin.^{6,7} These investigations showed that the acquisition of isotherm data requires caution, especially in the case of ionized compounds. The equilibrium constants depend on the activity coefficients of all the ions in the solution; i.e., the ionic strength of the solution must remain constant during each chromatographic experiment. This was achieved by using as the mobile phase a buffer having an ionic strength at least 10 times higher than the highest concentration of the component under study (here 1.1 mM). Under such conditions, the passage of the breakthrough front of the enantiomer does not significantly affect the activity coefficient of this compound in the mobile phase. Finally, the presence of adsorbed additives in the mobile phase might lead to system peaks but none were observed. The mobile phases used all contained 20.0 mM acetate ions and 20.0 mM sodium ions. In addition, they had different concentrations of undissociated acetic acid, depending on the pH. At the lowest pH (4.7), the mobile phase contained 20.0 mM acetic acid; at the highest pH (6.0), it contained 1.125 mM acetic acid.

c. Bi-Langmuir Adsorption Isotherm Data. The experimental results are reported in Figure 6a–c, in which the isotherms at the different pHs are plotted in the three different concentration ranges, respectively (symbols: \circ , (*R*)-propranolol; \ast , (*S*)-propranolol). In this Figure, the best isotherms obtained by fitting these experimental data to the bi-Langmuir model (eqs 4a,b) are also plotted (dashed lines, (*R*)-propranolol; solid lines, (*S*)-propranolol). The best values of the coefficients of the isotherm model are reported in Table 2.

d. The Isotherm Shapes. Figure 6a shows that, in the lowest concentration range, the isotherms of (*R*)- and (*S*)-propranolol are linear. There is only a minor deviation from linear behavior for the highest two isotherms (lines 5 and 6), corresponding to (*S*)-propranolol at pH 5.7 and 6.0. The influence of the pH is clear; at any given concentration, the amount adsorbed at equilibrium increases rapidly with increasing pH. The effect is stronger for (*S*)-propranolol than for (*R*)-propranolol, in agreement with the data obtained in the linear range by measuring the retention factors (Figure 2 and Table 1).

Figure 6b shows the data acquired in the intermediate concentration range. All the isotherms exhibit a nonlinear behavior. It is especially strong for (*S*)-propranolol, for which the curvature increases with increasing pH. The isotherms of (*R*)-propranolol are less strongly curved. At any mobile-phase pH, there is much less relative difference between the amounts of each enantiomer adsorbed at equilibrium in the high than in the low concentration range (cf. Figure 6a,b). Finally, in the high concentration range (Figure 6c), the isotherms of (*S*)- and (*R*)-propranolol corresponding to any given pH become close together. The resolution between the two enantiomers tends to disappear at high concentrations. The slopes of the isotherms

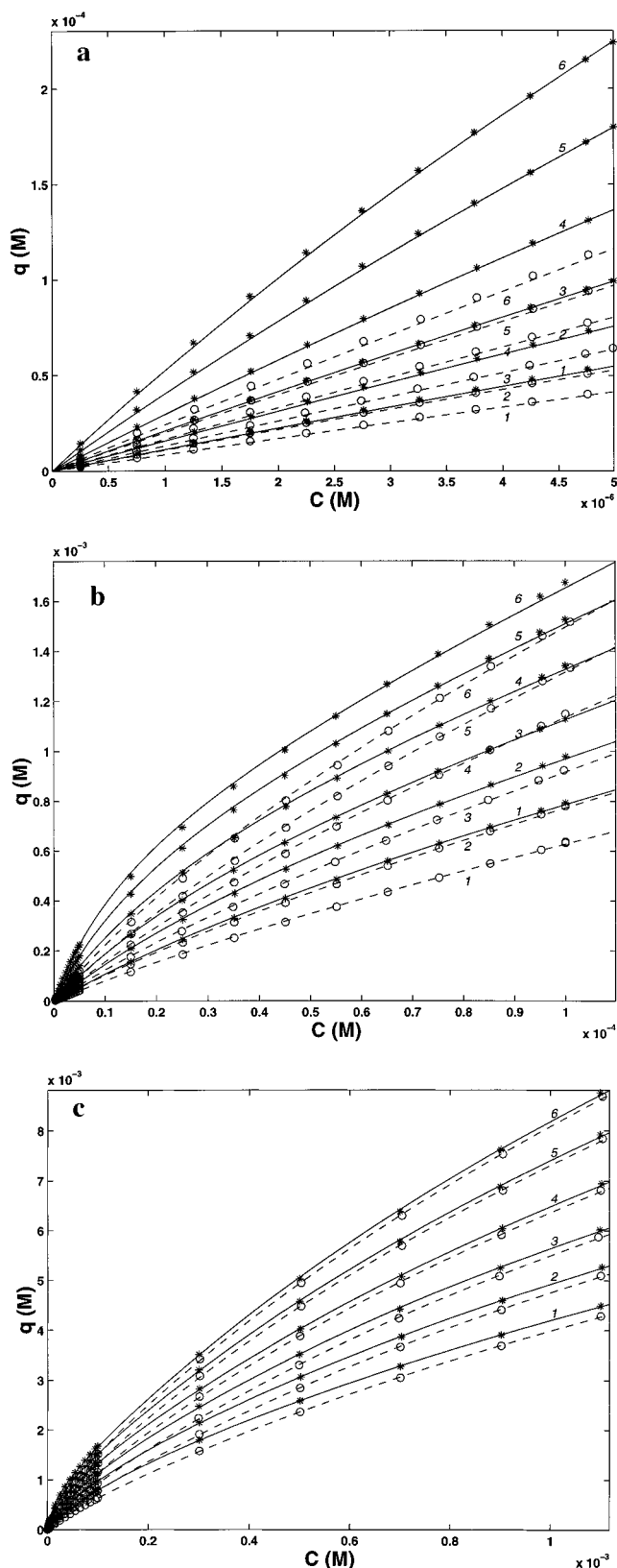


Figure 6. Single-component equilibrium isotherms for (*R*- and (*S*-propranolol at increasing pH. Experimental conditions are as in Figure 2. Symbols indicate experimental data: \circ , *R* enantiomer; $*$, *S* enantiomer. Lines are best calculated bi-Langmuir isotherms (parameters in Table 2): dashed lines, *R* enantiomer; solid lines, *S* enantiomer. Part a: low concentration range, between 0 and 5 μM ; pH values are (1) 4.72, (2) 4.98, (3) 5.21, (4) 5.49, (5) 5.70, (6) 5.93. Part b: medium concentration range, between 0 and 0.1 mM; pH values as in part a. Part c: high concentration range, between 0 and 1.1 mM; pH values as in part a.

are nearly the same and the distance between them becomes insignificant.

e. The Bi-Langmuir Parameters. These parameters are reported in Table 2. They were obtained by fitting each set of data to eq 4, with eight parameters, i.e., without introducing the assumption that the two enantiomers have the same coefficients for the contribution of type-I sites. This procedure allows the validation of our isotherm model. The a_I , b_I , and $q_{I,s}$ coefficients obtained for (*R*- and (*S*-propranolol are indeed very close, as should be the coefficients corresponding to nonchiral interactions. The coefficient a_I increases with increasing pH of the mobile phase. It is approximately twice as large at pH = 6.0 than at pH = 4.7. The coefficient b_I seems to increase slightly with increasing pH, an effect which is only barely significant given its small magnitude (ca. 16%) compared to the measurement error (rsd = 7%). This means that the increase of the coefficient a_I with increasing pH can be explained but partially by an increase of the energy of interaction of the enantiomers with the nonchiral sites. It is rather due to an increase of the column saturation capacity for the type-I sites. The coefficient $q_{I,s}$ increases by a factor of 1.8, from 15.4 mM at pH 4.7 to 27.6 mM at pH 6.0.

The parameters corresponding to the contribution of the interactions with the type-II sites, a_{II} , b_{II} , and $q_{II,s}$, are different for (*R*- and (*S*-propranolol. This is consistent with our adsorption model. For both enantiomers, the coefficient a_{II} increases rapidly with increasing mobile-phase pH. The effect is stronger for (*S*-propranolol, for which a_{II} increases nearly 7-fold when the pH is raised from 4.7 to 6.0, while for (*R*-propranolol the increase is only 4-fold (Table 2). The coefficient b_{II} of (*R*-propranolol increases only slightly with increasing pH (approximately by 12%). This means that the largest part of the increase in a_{II} originates from a 3-fold increase in the saturation capacity for (*R*-propranolol (Table 2). By contrast, b_{II} for (*S*-propranolol increases considerably with increasing pH, approximately 6-fold (Table 2). The column saturation capacity $q_{II,s}$ of the type-II contribution for (*S*-propranolol is nearly the same at low and high pH. Remarkably, its value, 0.80 mM, is nearly the same as the high-pH saturation capacity of (*R*-propranolol. So, the behaviors of the two enantiomers are most different. When the pH is increased, the number of enantioselective sites increases for (*R*-propranolol but remains constant for (*S*-propranolol. The energy of selective interactions remains constant for (*R*-propranolol but increases considerably for (*S*-propranolol.

These experimental results are illustrated in Figures 7 and 8 (note the two different scales: on the right for the nonselective parameter; on the left for the two enantioselective parameters). Figure 7 shows the dependence of the saturation capacities of the three retention mechanisms identified: the enantioselective interactions of (*S*-propranolol with type-II sites (line 1), those of (*R*-propranolol with the same sites (line 2), and the nonselective interactions of either enantiomers with type-I sites (line 3). Line 1 ((*S*-propranolol, type-II sites) is a nearly horizontal straight line, while line 2 ((*R*-propranolol, type-II) is a steep straight line. Line 3 (nonchiral type-I sites) is a steep straight line. Figure 8 shows similar plots for the thermodynamic constant of interaction, b . This time, lines 2 and 3 are nearly horizontal straight lines, while line 1 is a steep straight line.

f. Comparing the Bi-Langmuir Parameters and the Isotherms Shapes. The values of the parameters in Table 2 explain the observations made earlier regarding the distributions of the isotherms in Figure 6a–c. The initial slopes of the isotherms (Figure 6a) are the sums of the two coefficients a_I

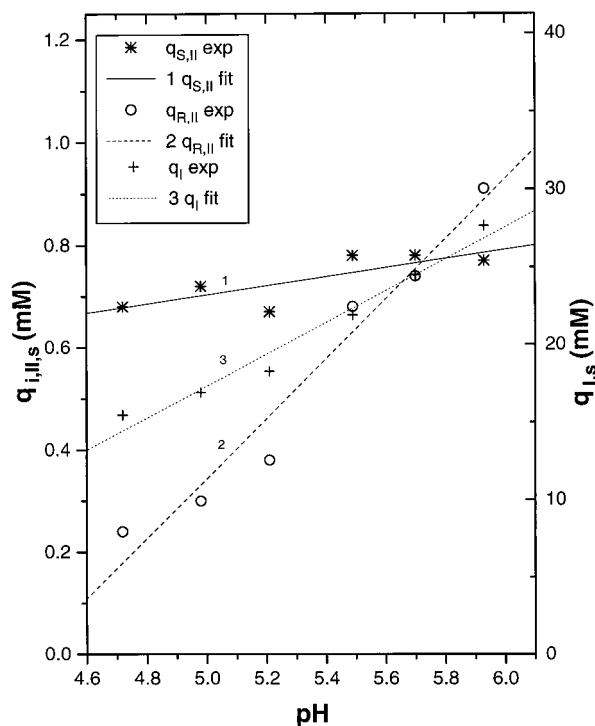


Figure 7. Plot of the saturation capacity of the three retention mechanisms versus the pH of the mobile phase: line 1, enantioselective interactions of (*S*)-propranolol with type-II sites; line 2, enantioselective interactions of (*R*)-propranolol with type-II sites; line 3, nonselective interactions of either enantiomers with type-I sites. NB. The left y-axis corresponds to lines 1 and 2; the right y-axis, to line 3.

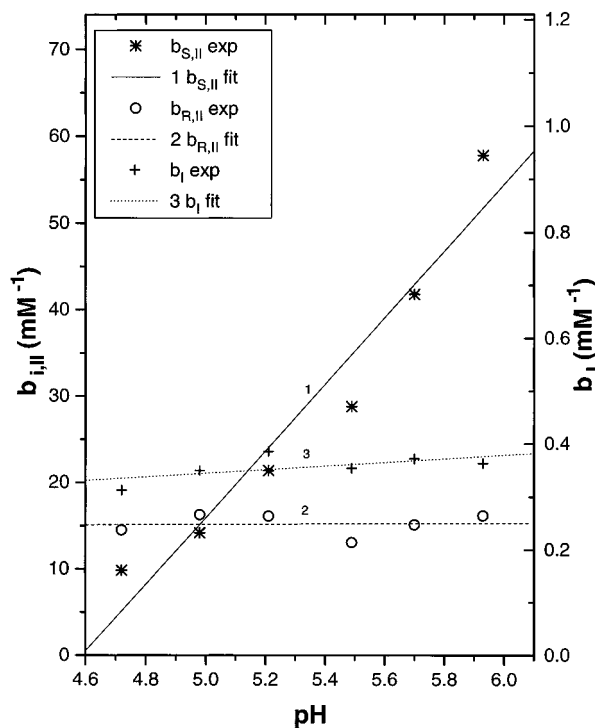


Figure 8. Plot of the binding constant of the three retention mechanisms versus the pH of the mobile phase: line 1, enantioselective interactions of (*S*)-propranolol with type-II sites; line 2, enantioselective interactions of (*R*)-propranolol with type-II sites; line 3, nonselective interactions of either enantiomers with type-I sites. NB. The left y-axis corresponds to lines 1 and 2; the right y-axis, to line 3.

and a_{II} . This sum is larger for (*S*)- than for (*R*)-propranolol. It increases much faster with increasing pH for the former than

for the latter enantiomer because of the large difference in the influence of the pH on a_{II} for the two enantiomers.

In Figure 6a, the experimental isotherms are linear because so are the contributions of the sites of both types. In Figure 6b, the influence of the curvature of the isotherm contribution of type-II sites to the experimental isotherm is important. The difference between the isotherms of (*R*)- and (*S*)-propranolol is explained by a comparison between Figures 5b (bottom right inset of Figure 5) and 6b. It is explained by the much larger value of b_{II} for the latter enantiomer. An increase of b_{II} causes an increase of the isotherm curvature in the intermediate concentration range. We have seen that b_{II} is nearly constant for (*R*)-propranolol but increases rapidly with the pH for (*S*)-propranolol. On the other hand, it was shown in the discussion of Figure 5b that an increase in $q_{II,S}$ causes an increase in the apparent slope of the isotherm, the effect observed for (*R*)-propranolol in Figure 6b.

In the high concentration range (Figure 6c), the type-II sites are practically completely saturated and adsorption follows essentially a Langmuir behavior, with a simple ordinate shift corresponding to the saturation of type-II sites. This explains why the isotherms are arranged in order of increasing pH, with a minor effect of the chirality, by contrast with what happens in the low and moderate concentration ranges. We also observe that, the higher the pH, the steeper the slopes of the (*R*)- and (*S*)-propranolol isotherms. This is due to an increase in the monolayer capacity of the type-I sites (cf. main Figure 4 and Figure 6c).

It was shown previously that the enthalpy of retention of (*S*)-propranolol was exothermic at pH = 4.66 and weakly endothermic at pH = 5.47.¹⁰ Note that, at pH = 5.49, b_{II} for (*S*)-propranolol becomes twice that for (*R*)-propranolol and $q_{1,II,S}$ ((*R*)-propranolol) becomes equal to $q_{2,II,S}$ ((*S*)-propranolol).

5. Enantioselective and Nonselective Mechanisms. The results presented in the previous sections are easily summarized. The retention factors of both (*R*)- and (*S*)-propranolol increase rapidly with increasing mobile-phase pH. The latter retention factor increases faster than the former, the separation factor also increases with increasing pH. These results are explained by the major role of the electrostatic interactions in both the nonchiral (type-I sites) and the chiral selective (type-II) interactions and by the increasing degree of dissociation of the acidic residues in CBH I, hence the increasing electrostatic interactions between the protein and the analytes. The strong pH dependence of the two retention factors is the result of the combination of three effects. When the pH increases, (1) the number of nonchiral type-I sites increases rapidly, (2) the monolayer capacity of the enantioselective sites for (*R*)-propranolol increases significantly, and (3) the binding constants of (*S*)-propranolol with these type-II sites increases considerably.

Our experimental results can be better understood in the light of results recently published on the three-dimensional structure of CBH I provided by X-ray crystallography.^{23,24} These results provide useful information regarding the origin of the changes of the properties of the type-I and type-II sites measured and reported earlier. The solute is an amino alcohol with a pK_a of 9.5. It is positively ionized in the whole pH range studied. The strongest interactions that can affect a cation are ion-binding to negatively charged groups of the stationary phase. These groups are in the protein, on its surface, or on the silica matrix. First, the residual silanols are becoming ionized in an increasingly large proportion with increasing pH in the range investigated. They all contribute to the nonselective interactions. Besides, the molecule of CBH I contains 43 carboxylic amino acid

residues, 24 aspartic acids and 19 glutamic acids. Sixteen acidic residues are located inside the tunnel, 11 aspartic acids and 5 glutamic acids. Most of the other acid residuals exist on the protein surface. Only a few are inside the protein globular structure. The pK_a values of the second carboxylic function of acidic amino acid residues of a protein molecule vary markedly, depending on their microenvironment, i.e., on the nature and position of close-by residues, and there is a rather broad distribution of pK_a for these groups. This suggests that a large fraction of them is not dissociated at $pH = 4.7$ but that most of them are at $pH = 6.0$. Thus, in this pH range, there is a considerable increase of the number of anionic charges on the protein molecules. This explains the important increase of the saturation capacity, $q_{I,S}$, of the type-I sites in our experiments.

Specific details of the structure of the tunnel inside the protein were supplied by the same X-ray crystallographic study.^{23,24} They suggest that the enantioselective sites would involve essentially the carboxylic groups of two glutamic acid residues and the hydrophobic indole ring of a tryptophan residue.^{27–29} This assumption is validated by the observation that the ratio of the number of carboxylic groups in the active site to their total number in the protein is 22, while the ratio of the nonselective to the *S* enantiomer selective saturation capacities varies from 23 at $pH = 4.72$ to 36 at $pH = 5.93$ (cf. Figure 7). Obviously, not all nonselective interactions can be ascribed to ionic interactions between carboxylate groups and the positively charged nitrogen atom on the propranolol. There are other type-I sites, e.g., the dissociated silanol groups at the silica surface or the so-called silanophilic and hydrophobic interactions.¹⁰ However, the dependence of this capacity on the pH suggests that these ionic interactions play a very important role. If the active site has the postulated structure, the increase of the energy of binding, $b_{2,II}$, of (*S*)-propranolol to the enantioselective type-II sites (cf. Figure 8) should be related to the influence of the pH on the degree of ionization of the two carboxylic groups at the selective site. The presence of the positively charged nitrogen atom between them mitigates their electrostatic repulsion and might cause the loss of the solvated water molecules, hence the large adsorption entropy.¹⁰ Because (*R*)-propranolol does not fit well to the selective site, the increased ionization of the carboxylic group has little effect on its selective binding constant but simply makes more sites available for interaction. This explains the increase of its saturation capacity for the selective sites while its binding constant is little affected.

In this context it should be mentioned that, although ionic interactions play a dominant role, we did not try to model the isotherm data with one of the several stoichiometric or non-stoichiometric models available,^{33,34} examples of the latter being the several versions of the Stern–Gouy–Chapman (SGC) theory concerning the electrical double layer.^{33,34} These models are based on the Langmuir model³⁴ but are more flexible because of the higher number of parameters needed to account for the electrostatic interactions at the microscopic level. There is a limit to the amount of information that can be extracted from chromatographic data, and it seemed more useful to concentrate

on the separation between the contributions of the enantioselective and nonselective interactions. This made more attractive the use of the semi-empirical bi-Langmuir model.

Conclusions

The results reported here confirm and extend our previous findings regarding the chiral separation of the enantiomers of a β -blocker on an immobilized protein.¹⁰ Combined with recent results of X-ray crystallography unraveling the structure of CBH I, our experimental measurements of the adsorption data of (*R*)- and (*S*)-propranolol have allowed the first detailed description of the enantioselective site.

Furthermore, these results permit the derivation of a systematic procedure for the investigation of enantioselective retention mechanisms. The measurement of the adsorption data of the two enantiomers studied on the selected CSP followed by the modeling of these data using the bi-Langmuir isotherm allows the direct determination of the nonselective and the enantioselective contributions to the retention of these compounds. From these contributions, the values of the saturation capacity and the binding constants of the two enantiomers on the nonselective type-I sites and each of them on the enantioselective type-II sites can be derived. The access to these thermodynamic characteristics of the different interactions taking place on CSPs allows a detailed investigation of the retention mechanism. The study of the influence of the temperature, of the mobile-phase pH , and/or of any relevant parameter on these constants will be particularly informative, especially if details of the CSP composition and structure are available and permit the interpretation of the thermodynamic data.

This methodology has proven successful in a number of different instances.^{6–10} In only one case, did the bi-Langmuir isotherm prove to be an unsuitable model.³² The information gained when more sophisticated models are needed is extremely valuable. Its interpretation will become possible only when further progress is made in the modeling of weak intermolecular interactions.

In the case of the separation of (*R*)- and (*S*)-propranolol on immobilized CBH I, we have also shown that the parameters of the isotherm which describes the nonselective adsorption depend only weakly on the pH of the mobile phase. By contrast, the parameters of the enantioselective adsorption isotherm depend strongly on the pH , suggesting that the corresponding mechanism is mainly ionic. Comparison with the results of independent studies on the X-ray structure and the enzymatic activity of the protein allowed a plausible suggestion regarding the identity of the groups of atoms which carry the chiral selectivity.

Acknowledgment. This work was supported in part by Grant CHE-9701680 from the National Science Foundation and by the cooperative agreement between the University of Tennessee and Oak Ridge National Laboratory. We acknowledge the support of Maureen S. Smith in solving our computational problems and thank the Swedish Natural Science Research Council (NFR) and Astra Hässle AB (Mölnådal, Sweden) for financial support of this project.

(33) Chen, J.-G.; Weber, S. G.; Glavina, L. L.; Cantwell, F. F. *J. Chromatogr.* **1993**, 656, 549.

(34) Häggglund, I.; Ståhlberg, J. *J. Chromatogr., A* **1997**, 761, 3.